

The Effects of Sputtering Energy regarding Defect Formation on the Ge(110) Surface as Observed through Scanning Tunneling Microscopy

Samantha MacIntyre
Shippensburg University

In Collaboration with Dr. Shirley Chiang, Marshall van Zijll, Bret Stenger, Michael Norton and Noelle Oguri, UC Davis

Abstract: The effects of sputtering on Ge(110) is investigated through the use of scanning tunneling microscopy. Through the adjustment of beam energy the sputtering effects on the surface become prevalent over time resulting in the formation/emergence of pyramid structures on the surface. This study aims to understand the impact of sputtering on the sample with special attention given to the formation of pyramid structures on the surface as well as their size and density on the surface.

1. Introduction

Technological advancement has changed our world drastically. As our devices become more complex and shrink in size, the need for clean, homogeneous substrate surfaces increases. By studying a material's surface structure, we observe many new phenomena, such as the occurrence of surface reconstruction, in which the crystallographic structures on the surface can be very different from the bulk structure. Sample cleaning is a common precursor to both bottom up, and top down manufacturing, the methods of producing the semiconductor devices for modern technology. A typical cleaning technique, occurring under ultrahigh vacuum (UHV) conditions involves the use of a sputtering gun. The surface is bombarded by argon atoms from the sputtering gun, physically knocking off surface contaminants, then the sample is heated (annealed), to just below the melting point, allowing for the crystal structure to repair itself. This common technique is used widely, and the presence of persistent surface features in past studies motivated this study. Pyramid structures in Ge(110) have been observed in the past, although the exact formation mechanism is unknown.

2. Apparatus

This experiment is performed in a cluster tool comprising of x-ray photoemission spectroscopy (XPS), scanning tunneling microscopy (STM), and low energy electron microscopy (LEEM). The entire system is kept under UHV pressures on the order of 10^{-10} torr, and the samples can be transferred throughout the UHV chambers employing manipulators and transfer bars ensuring that the sample is never removed from the vacuum environment during the experiment. This is a crucial matter, because the experimental premise is based on cleanliness. This experiment utilizes only the XPS chamber for cleaning cycles, and the STM chamber for characterization.

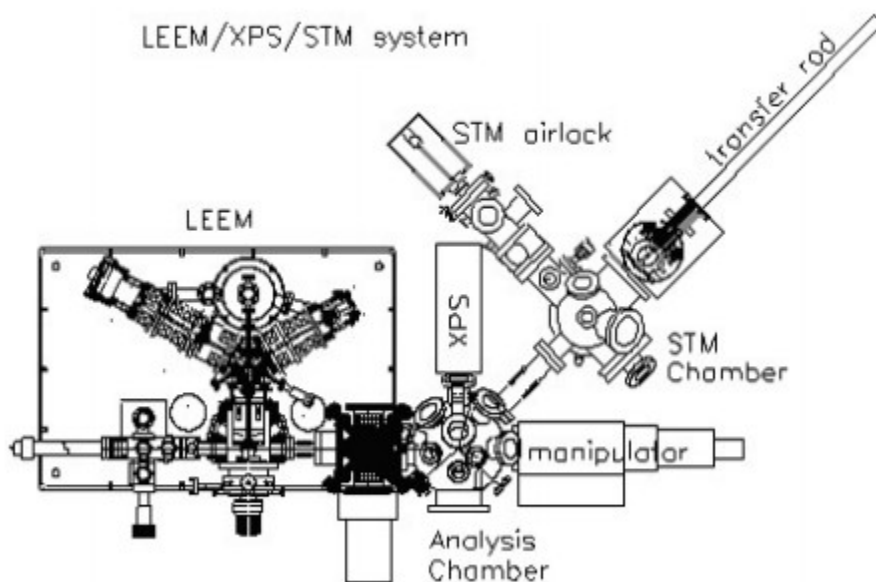


Figure 1: Diagram of the U.C. Davis LEEM/XPS/STM system. The entire system maintains UHV around $10^{-9} - 10^{-10}$ torr. The entire cleaning and imaging process takes place without ever leaving the vacuum environment. Cleaning occurs in the XPS analysis chamber and imaging occurs in the STM chamber. ⁱ

The primary characterization method of STM dates back to 1981, invented by Binnig and Rohrer, who later became Nobel Laureates in 1986 for their creation. The STM relies on the phenomenon known as quantum tunneling. An atomically sharp tip is positioned extremely close to the surface of the sample, and a bias is applied between the tip and sample inducing a tunneling current between them; the tunneling current. The tip is mounted in a way that allows piezoelectric materials to control the movement of the tip. The tip scans the surface in a raster pattern and through the use of a feedback loop, the tool keeps either the working distance, or the tunneling current constant, allowing topographic information of the sample surface to be acquired and displayed. For the purposes of this experiment, the tunneling current is kept constant and the tip directly mimics sample topographic structure. The software program WSxM is used to analyze raw images through flattening, contrasting, obtaining profile information and zooming/cropping. WSxM is a powerful tool for use with not just STM, but also for use with many other scanning probing microscopy (SPM) techniques.

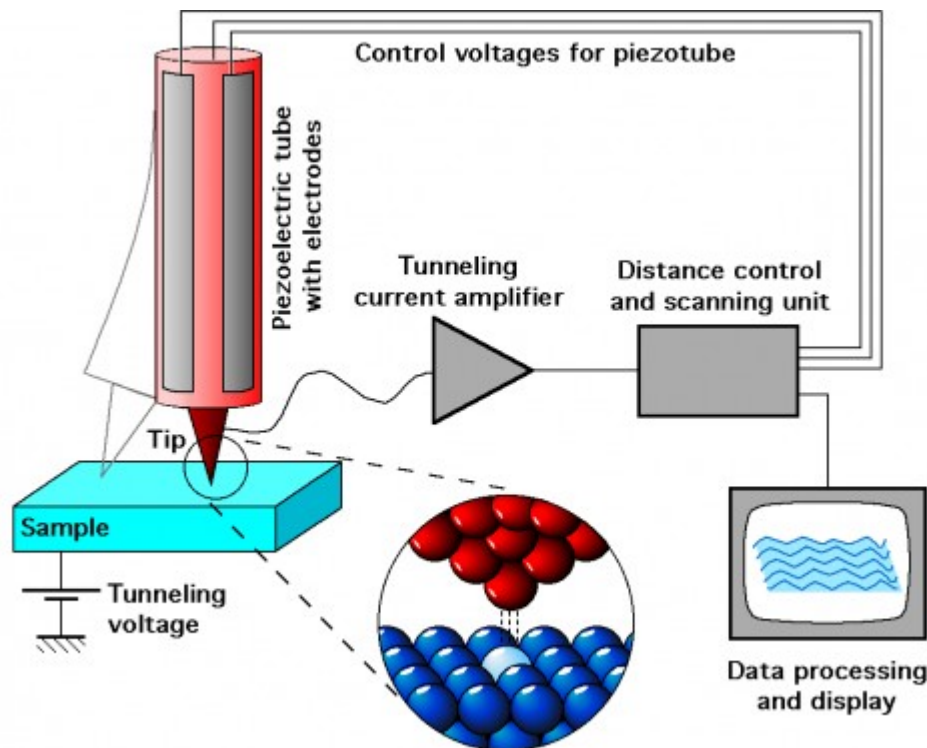


Figure 2: STM general working principles. The atomically sharp tip is held close to the surface, and controlled by high sensitivity piezoelectric materials. The tip is rastered across the surface and the changes in tunneling current are measured and result in a display of topographical information of the surface at atomic resolution. Figure reproduced with permission by Michael Schmid, TU Wien.

Due to the exponential dependence of the tunneling current and the working distance, the depth resolution of the STM is incredible; on the order of 0.01nm.ⁱⁱ This relationship is evident through this approximation to the tunneling current equation

$$I = Ve^{-A\sqrt{\Theta}d}$$

In this equation, I is the tunneling current, V is the bias voltage, A is a constant, Θ is the average workfunction between the tip and sample, and d is the tip to sample distance. This approximate equation demonstrates the distance dependence of the tunneling current, verifies that Ohm's law holds, and accounts for chemical effects through the workfunction (Θ).

The lateral resolution is limited by the electronic structure of the surface and is on the order of 0.2nm.ⁱⁱⁱ This resolution makes the STM capable of atomic resolution, imaging single atoms! This image capability is important to surface physics, giving visual representation of surface crystal lattices.

3. Experimental Procedure

The cleaning technique is fairly straight forward. The sample is placed in the XPS chamber, which is backfilled with argon gas, and aligned for sputtering. Argon gas is ionized in the sputtering gun and accelerated towards the sample, which is grounded. The argon ions then bombard the sample surface, utilizing their kinetic energy to knock off surface contaminants. The incident argon beam is approximately normal to the sample surface. This beam is maintained for 15 minutes, with emission

current kept within the range of 10mA-15mA and beam energies varied experimentally between 0.1keV and 0.4keV.

Once the sputtering step is complete, the sample is then thermally annealed through electron bombardment heating. A 2.7A current is passed through a filament beneath the sample, emitting electrons which are attracted to the sample through an applied potential difference of between 100-300V, and heating the sample up to 800 C - 850 C. This step takes 10 minutes, and with the completion of the annealing, the sample has finished one cycle of cleaning.

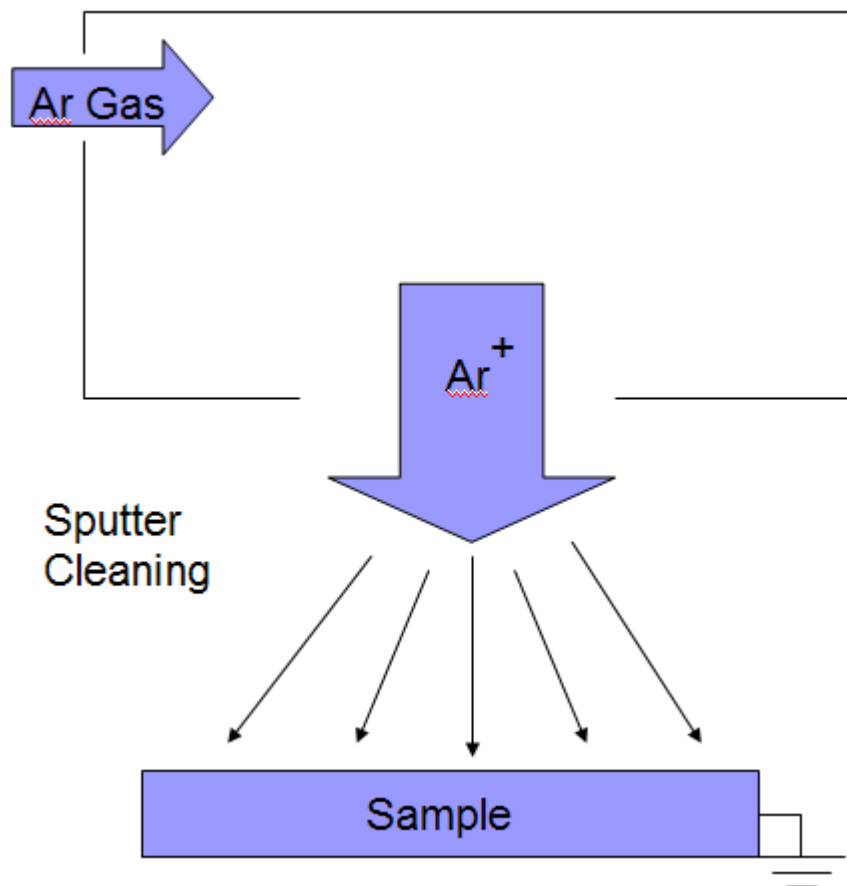


Figure 3: Sputtering involves the ionization of argon gas in a sputter gun. Current is run through a filament in the gun which then induces thermionic emission of electrons. The electrons are attracted to a positively biased area in the gun, on the way ionizing the argon gas. The ionized Argon is repelled from the positive bias, out of the sputter gun towards the grounded sample. When the ionized argon collides with the sample, the kinetic energy of the bombardment physically knocks off contaminant layers leaving the sample cleaner, but damaged.

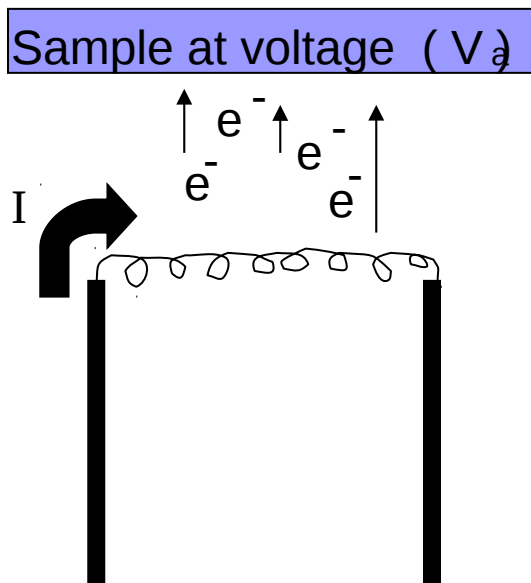


Figure 4: The thermal annealing step is achieved through electron bombardment heating. Below the sample, within the sample holder, a heating filament is located within a reflector cup. Current (2.7A) flows through the filament inducing thermionic emission of electrons. A voltage of between 100V to 300V is placed on the sample, and this potential difference directs electrons to strike the back of the sample. The energy the electrons impart to the sample heat it in a reliable and controllable manner.

The experimental procedure holds all variables constant except for beam energy. A Ge(110) sample is obtained and placed in the UHV chamber where it is sputter cleaned using the argon ions with 0.1keV beam energy, and characterized by STM at various cycle intervals. Then, a new sample is cleaned using the 0.2keV and again characterized by STM at various intervals, another sample goes through the same process at 0.3keV, and then the final sample at 0.4keV. This procedure ensures that the results are based entirely on the variation in beam energy at each level, without relying on previous cleaning methods, at lower energies. Upon characterization, scans are taken and analyzed based on current knowledge of the typical surface structure of Ge(110). The sample surface is scanned, and images are saved of all scans. The important surface features which identify clean Ge surfaces are $c(8 \times 10)$ surface reconstruction and faceting. Other features of interest are the pyramidal structures which have been observed previously in this laboratory.

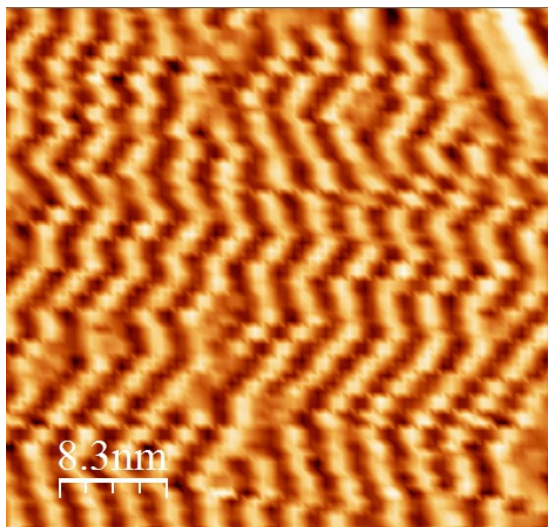
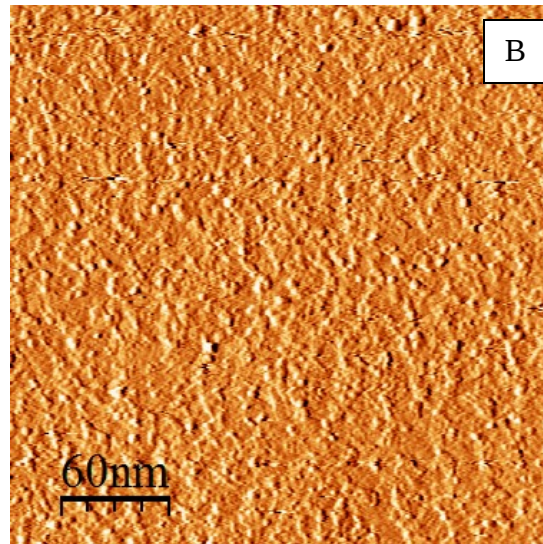
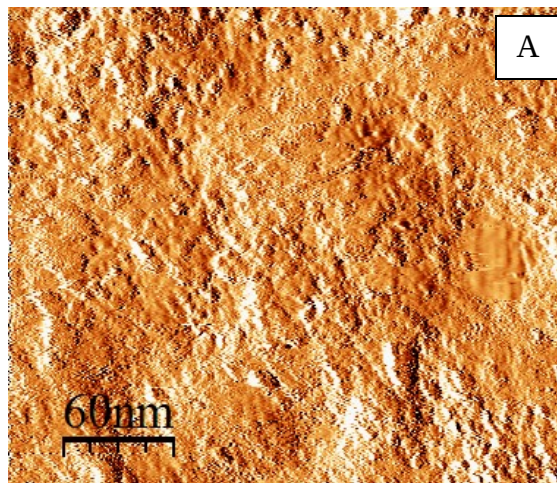


Figure 5: The $c(8 \times 10)$ structure of Ge(110) is seen here. This pattern of zigzag rows allows us to reliably affirm that the image we are seeing is actually of the clean Ge(110) surface, and not a contaminant layer.

4. Experimental Results

4.1. 100eV

At 100eV, we obtained reasonable, consistent results regarding the cleanliness of our surface, and the possible emergence of pyramids. With low energy sputtering and low cycles of cleaning, we found predictably that our surfaces were still quite dirty and contaminated.



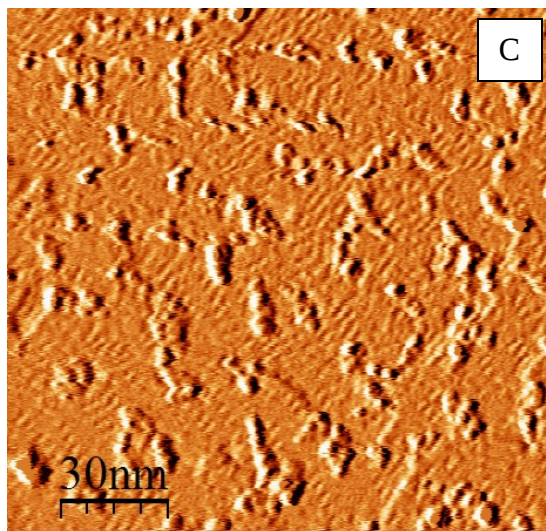


Figure 6: STM images of Ge(110) surface, cleaned with 100eV argon ions and varying numbers of cleaning cycles. (A) 8 cycles.(B) 14 cycles. There is no evidence of structured $c(8 \times 10)$ Ge(110), implying that the samples are still quite dirty, covered in a film of non-ordered contamination. (C) 23 cycles. Between the large protrusions, there is evidence of surface ordering in the preferred $c(8 \times 10)$ pattern.

The sample did eventually attain a level of cleanliness where there was clear evidence of the Ge(110) surface through the observable $c(8 \times 10)$ surface reconstruction. Although there was no concrete evidence of pyramids at this energy level, there is a possibility that a surface feature we imaged may be a pyramid precursor. Typically, our pyramids are oriented in such a way that a side is parallel to a preferred faceting direction within the Ge(110) surface itself, and in conjunction with this, the pyramidal structure is surrounded by faceting making it clearly distinguishable.

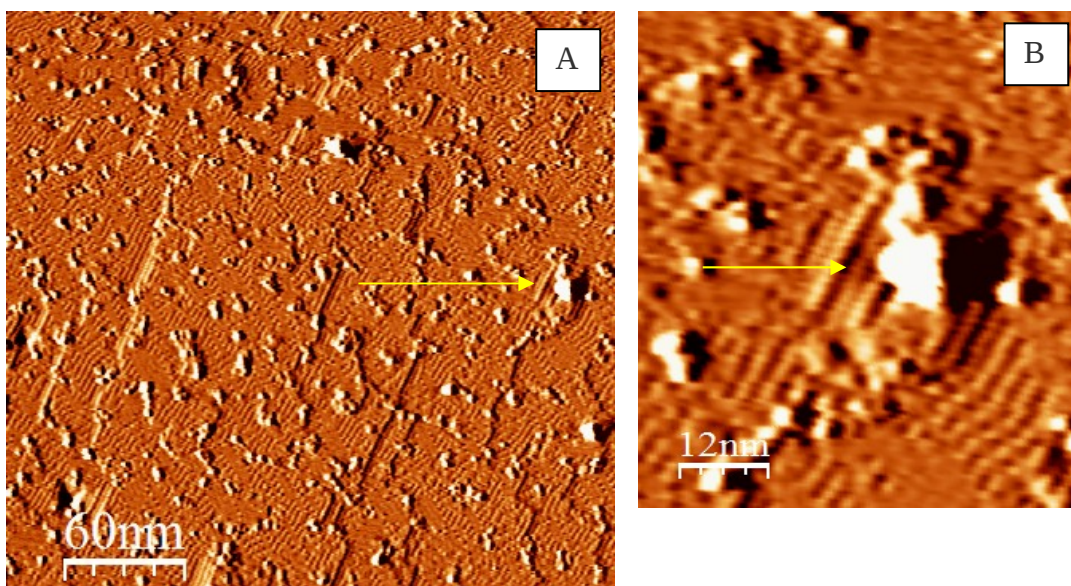
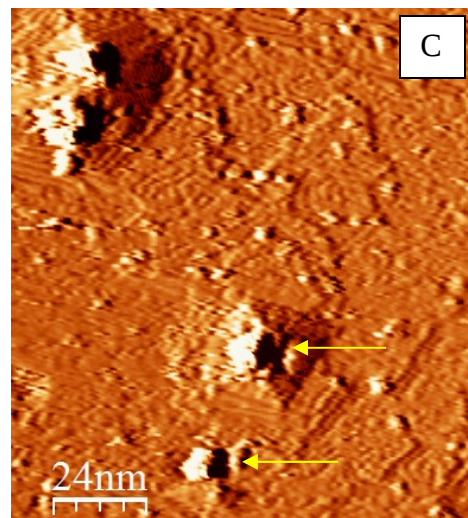
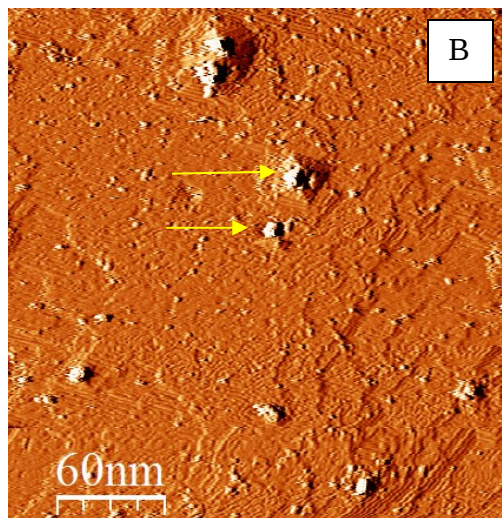
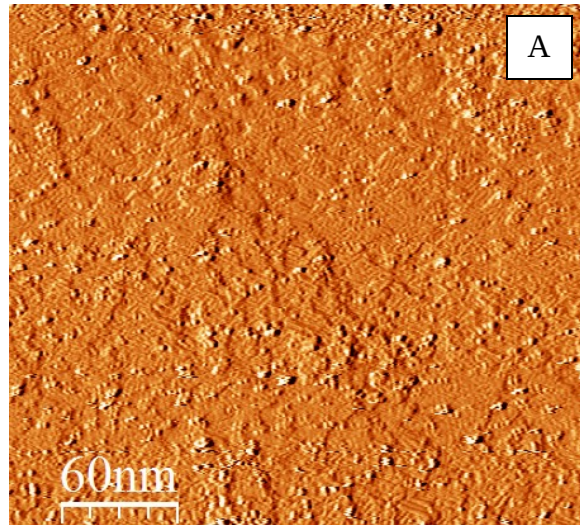


Figure 7: STM images of Ge(110) cleaned at 100eV for 33 cycles. The yellow arrow points to the surface feature of interest. This feature appears to be surrounded by faceting which is present for pyramids observed previously. Again, this is not conclusively a precursor pyramidal feature. At 100eV, there were no confirmed pyramids, but these “baby” features were present in many of our scans.

4.2 200eV

At 200eV, our images were marked by easy identification of pyramidal structures, as well as possible recognition of pyramid precursors and developing structures. It is interesting to note that the size of the possible pyramid precursors, and the size of the odd, non-faceted feature located at the top of all of our pyramids are approximately the same. This size comparison is evident in Figure 8 (B) and (C) where the embedded blob appears similar in shape and size as the blob on top of the pyramid, both features being marked by yellow arrows.



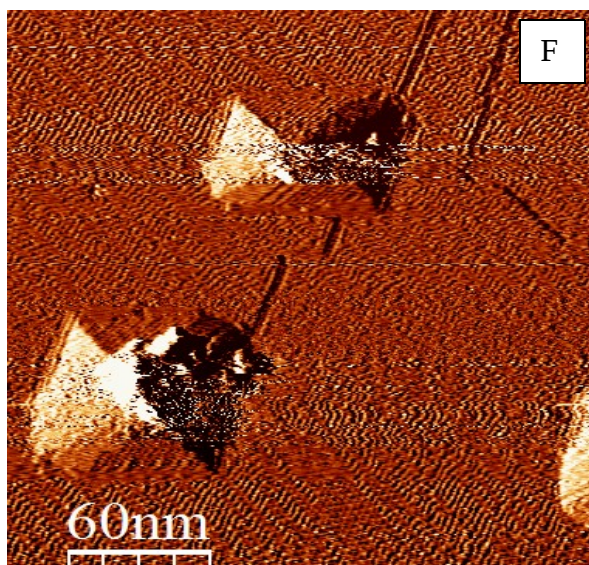
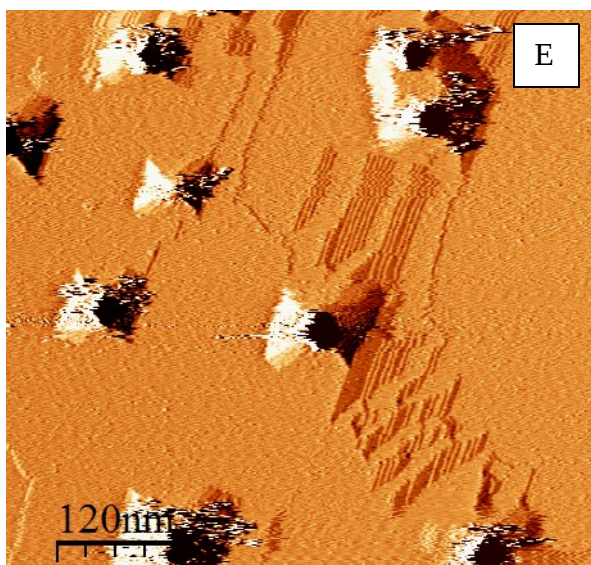
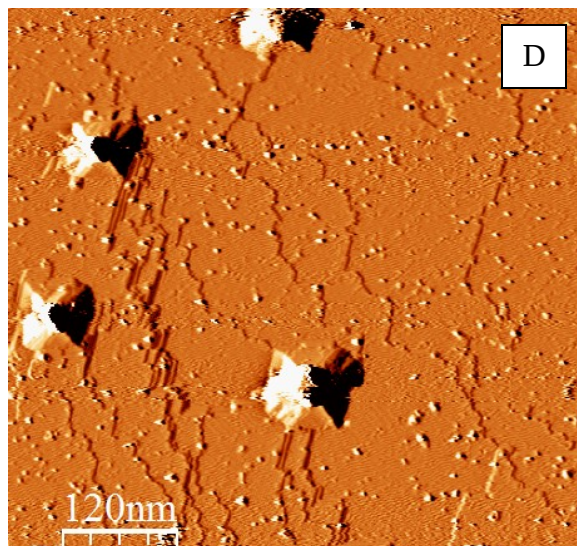


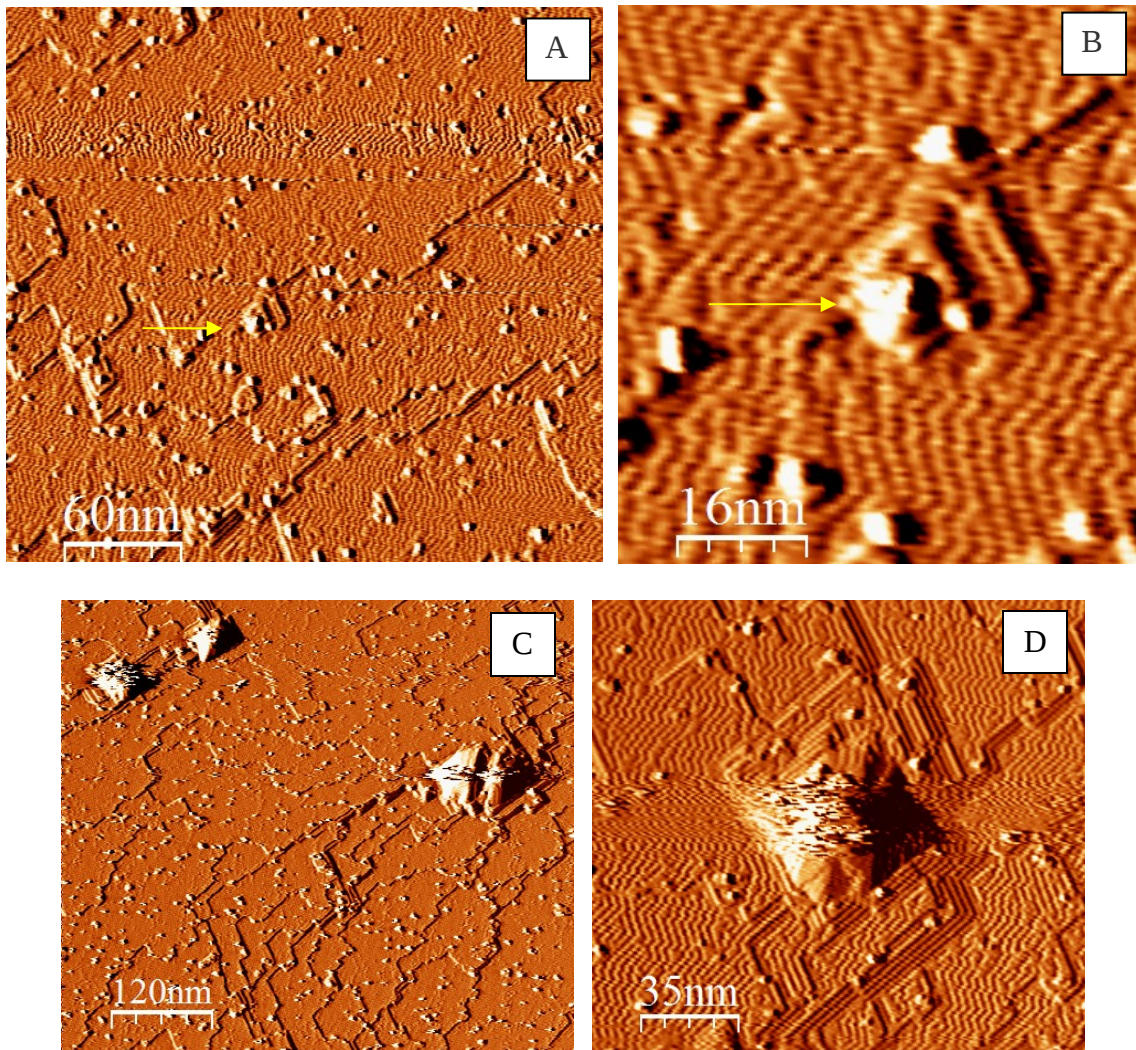
Figure 8: STM images of Ge(110) samples with argon sputtering at beam energy of 200eV. (A) 9 cleaning cycles, showing a dirty surface. (B) and (C) 14 cycles, with clear evidence of pyramids. C is a close up of the top two pyramids in B. It is interesting to note that the surface features indicated by yellow arrows are similarly shaped and sized, giving evidence for the surface feature to be a precursor to developing pyramids. (D) cleaned 18x, showing four more pyramids. (E) and (F) cycled 40 times, showing massive-sized pyramids, with a high density of pyramids per image. Image E also serves as a great example of how the pyramids are oriented. Pyramids orient themselves in such a way that one side is parallel to the preferred faceting of the sample. The series of long straight lines in (E) are typical Ge(110) faceting.

Imaging our sample sputtered at 200eV provided us with a large amount of pyramid data. The pyramids were very common on our sample surface and had grown quite large by the end of our cleaning cycles. The size of the pyramid features proved to be a hazard for our STM tip; however, we were still able to produce some images with extremely high resolution.

4.3 300eV

At 300eV, our images were marked by an incredibly sharp tip, producing the best resolution we have seen all summer. They also reminded us that science does not always follow your initial intuition. At

this point, we have not yet completed our experiments in the 300eV range, and thus it is our last set of data for analysis. The most interesting observations concerning the images of the sample cleaned at 300eV is that there are fewer pyramids than found at 200eV, they are widely spaced, and the ones we did find were degraded in some fashion. The ones we did find were after exhaustive effort, with many 600nm scans showing no pyramids at all. This indicates to us that there is more going on than with the emergence of these structures than previously thought, and that there is still much to learn about the dynamics of pyramid formation and how sputtering affects it



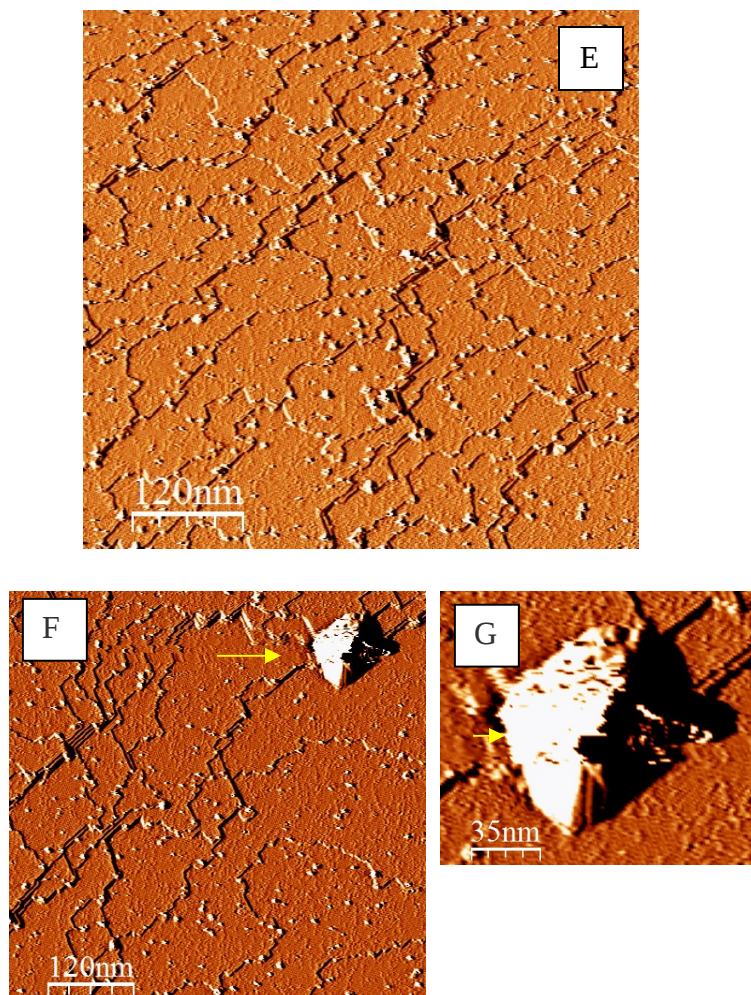


Figure 9: STM images were Ge(110), after argon ion sputtering at 300eV. (A) and (B) underwent 7 cycles, and the yellow arrow points to a surface feature believed to be a pyramidal precursor. (C) and (D) were cycled 13 times. It is interesting to note that these pyramids appear broken down and messy compared to pyramids found when sputtering with 200eV argon ions.. (E), (F) and (G) were all taken after the sample had completed 19 cycles. Aside from the extremely large structure in image (F) and highlighted in (G), there are relatively few pyramidal structures.

5. Experimental Conclusions

Although we cannot make definitive conclusions at this stage of our experiment, we can suggest a few possibilities. Once the 300eV scans are completed, and we finish the 400eV scans, work can begin on quantifying the pyramid size and surface abundance. When this experiment first began, it was believed that with higher beam energy, pyramids would get bigger and would have a higher density per unit area on the surface. Once imaging at 300eV began and we saw fewer pyramids, we began to suspect an energy threshold for pyramid formation. It is my belief that pyramids in Ge(110) form as a result of uncovering a crystal defect already existing in the sample. This crystal defect may propagate down into the germanium. By sputtering away layers of germanium, the pyramid may form out of a preferred, faceting pattern based on bonding energy and orientation. If such a phenomenon occurs, than there is the chance that when bombarded with ions of high enough energy, uncovered pyramids will degrade and possibly even become eradicated completely. This would explain the low appearance of pyramids at the 300eV level.

6. Acknowledgments

My acceptance into the University of California, Davis's 2012 Summer REU program has presented me with the incredible opportunity to participate in real and innovative research, the likes of which I would not have access to at my home school. This valuable experience will be a powerful tool and advantageous when I enter into a graduate program in my future.

I am so grateful for this experience, and I have many people to thank for making it possible for me to be here. I'd like to thank Dr. Shirley Chiang, for choosing me despite having never met me, and for providing me with a seemingly endless supply of reading material at all levels to aid my understanding of solid state physics. Immediately her expertise and intelligence became a welcome aid in my endeavor to begin to comprehend the complexities of surface science. I'd also like to thank Marshall Van Zijll and Bret Stenger for including me in their research projects, and always taking time to answer my limitless battery of questions about the tools, the samples, and pretty much anything and everything that came to mind during my time in the lab. They provided a fun atmosphere to work in, and were so incredibly accommodating. Along with Marshall and Bret, I'd like to thank the undergraduates Michael Norton and Noelle Oguri, to whom I wish the best of luck. Deserving thanks as well are the Physics and Math Department faculty at Shippensburg University for countless letters of recommendation and support through the whole process. Dr. Rena Zieve was an incredible coordinator for the program, and I'd like to thank her for the time she spent preparing us for the GRE and planning fun group outings. Finally, I'd like to thank the NSF for providing the grant funding allowing for this program to take place.

This program has piqued my interest in experimental solid state physics. With the rapid improvement of technology, characterization has become an invaluable tool. My interest in surface modification and materials science go hand in hand with surface characterization methods. What I have learned from this program will stay with me throughout my career.

- i C.L.H. Devlin, D.N. Futaba, A. Loui, J.D. Shine, S. Chiang, "A Unique Facility for Surface Microscopy," *Materials Science & Engineering* **B96**, 215-220, (2002).
- ii G. Binnig, H. Rohrer, *Scientific American*, **25** pp. 40-46. (1985)
- iii Prutton, M. *Introduction to Surface Physics* Clarendon Press, Oxford, pp 90-92. (1994)